AGU PUBLICATIONS

JGR

Journal of Geophysical Research: Space Physics

RESEARCH ARTICLE
10.1002/2015JA021406

Special Section:
Variability of the Sun and Its Terrestrial Impact VarSITI

Key Points:
- Extreme 23 July 2012 solar event simulated with HAFSS 3-D time-dependent model
- Results agree with spacecraft data from 1 AU, the heliosheath, and beyond
- Results show important physical phenomena consistent with metaphorical tsunami

Correspondence to:
D. S. Intriligator,
devriei@aol.com

Citation:
Intriligator, D. S., W. Sun, M. Dryer, J. Intriligator, C. Deehr, T. Detman, and W. R. Webber (2015), Did the July 2012 solar events cause a "tsunami" throughout the heliosphere, heliosheath, and into the interstellar medium?, *J. Geophys. Res. Space Physics*, *120*, 8267–8280, doi:10.1002/2015JA021406.

Received 30 APR 2015
Accepted 20 SEP 2015
Accepted article online 28 SEP 2015
Published online 27 OCT 2015

Did the July 2012 solar events cause a "tsunami" throughout the heliosphere, heliosheath, and into the interstellar medium?

Devrie S. Intriligator[1], Wei Sun[1,2], Murray Dryer[1], James Intriligator[1,3], Charles Deehr[2], Thomas Detman[1], and William R. Webber[4]

[1]Carmel Research Center, Santa Monica, California, USA, [2]University of Alaska, Fairbanks, Alaska, USA, [3]Bangor University, Bangor, UK, [4]New Mexico State University, Las Cruces, New Mexico, USA

Abstract The July 2012 major solar events gave rise to manifestations observed at many longitudes/latitudes/radial locations throughout the heliosphere, heliosheath, and into the interstellar medium. For these solar events we present our initial results at 1 AU from our HAFSS (Hakamada-Akasofu-Fry Source Surface) three-dimensional time-dependent kinematic modeling. Our simulations, using Wang-Sheeley-Arge maps and solar event observations, start at 2.5 R_S from the center of the Sun. We use both the quiescent background solar conditions and the solar events (e.g., coronal mass ejections (CMEs)) as inputs and propagate outward. We compare HAFSS predictions with in situ spacecraft measurements and conclude that the July 2012 solar events caused a metaphorical "tsunami" in the plasma and magnetic field throughout the heliosphere/heliosheath/interstellar medium. The simulations show evidence of shocks, interaction regions, and rarefaction regions in the inner heliosphere (1 AU) and shocks, global merged interaction regions (GMIRs) and rarefaction regions in the heliosheath. The shocks/interaction regions/GMIRs and the rarefaction regions are, respectively, analogous to the tsunami "crests" and "troughs". To provide important insights into 3-D processes, we simulated 1 AU observations (STEREO A and ACE) and observations at Voyager 2 (V2) and Voyager 1 (V1) far off the ecliptic plane: V2 at ~30°S, 217° longitude, and 102 AU; V1 at 34°N, 174° longitude, and 124 AU. HAFSS successfully predicted observed CME arrival times at 1 AU. Our results for this tsunami are the first simulations for these events in the distant V2/V1 radial/latitudinal/longitudinal regions based on 3-D time-dependent modeling originating at the Sun.

1. Introduction

The solar minimum between solar cycles 23 and 24 can be characterized as "quiet" and "deep" in comparison to those between the recent previous solar cycles. It was quiet in that there were very few interplanetary (IP) events of solar origin. It was deep in that the magnitudes of the solar magnetic field and the interplanetary magnetic field (IMF) near Earth were substantially lower than those observed in previous recent solar minima. The end of the solar minimum was well observed at 1 AU by the ACE, STEREO A, and STEREO B spacecraft (s/c) that were at various longitudes around the Sun [*McComas et al*., 2013]. In addition, there were remote sensing observations of the Sun from the Solar Dynamics Observatory s/c and from SOHO (Solar and Heliospheric Observatory) [e.g., *Howard et al*., 2008].

As solar activity slowly resumed this fleet of s/c observed relatively few and modest solar events, e.g., September 2011, January 2012, and March 2012. Thus, it was somewhat surprising when the large and powerful July 2012 solar events occurred. *Shen et al*. [2014] studied the 12 July 2012 solar event. This was followed by a series of solar events from 17–23 July 2012. *Dryer et al*. [2012], *Russell et al*. [2013], *Liou et al*. [2014], and *Wu et al*. [2013] each studied some of these events. In the present paper we analyze the 17–23 July solar events. Much has been made of the L1 magnitude of the 23 July 2012 solar event at STEREO A. At this s/c the magnitude of the 23 July 2012 solar event was considered comparable to or even greater than the 1859 Carrington events [*Baker et al*., 2013]. The details of the extreme nature of this event were described by *Dryer et al*. [2012], *Ngwira et al*. [2013], and *Liou et al*. [2014]. *Mewaldt* [2014], *Russell et al*. [2013], and others attributed the sometimes fairly modest IP solar wind (SW) and IMF observations associated with the 23 July 2012 solar event at 1 AU to the effects of the solar energetic particles (SEPs). That is, the SEPs mediated the shock [*Florinski et al*., 2009]. At times the SEP pressure exceeded the magnetic pressure by a factor of ~70.

Table 1. July 2012 Solar Events and HAFSS Model Inputs

YYYY	MMDD	HHMM	LAT	LON	VS	TAU	VSW	OPT	XRAY
2012	0717	1354	S23	W061	802	0300	750	XXX	XXX
2012	0718	0624	N18	W180	713	0300	750	XXX	XXX
2012	0719	0539	S17	W092	1106	0300	750	XXX	XXX
2012	0723	0250	S16	W133	3603	0330	750	XXX	XXX

In the present paper we report the results of our analyses at 1 AU in the ecliptic plane and in the heliosheath (HS) and interstellar medium (ISM) in the vicinity of Voyager 1 (V1) and Voyager 2 (V2). V1 and V2 were located, respectively, at 30°N and 34°S of the ecliptic plane. We used the HAFSS (Hakamada-Akasofu-Fry Source Surface) model [*Intriligator et al*., 2008, 2010, 2015] that we developed (see below) to analyze the heliospheric, HS, and ISM propagation of the 17–23 July 2012 solar events. HAFSS is a three-dimensional (3-D) time-dependent kinematic model originating at the Sun that simulates the quiescent (background) SW and the disturbed SW. We compared the HAFSS predictions with the available s/c data. The HAFSS model and solar events are discussed in section 2. The following two sections, 3 and 4, discuss the HAFSS model comparisons with the 1 AU and HS/ISM measurements, respectively. In section 5 we discuss our results and conclusions.

2. The HAFSS Model

The HAFSS (Hakamada-Akasofu-Fry Source Surface) model [*Intriligator et al*., 2008, 2010, 2015], a 3-D kinematic time-dependent model, is suited for these analyses since it simulates the slowly evolving background SW starting from the Sun and the impulsive, time-dependent events associated with solar activity (e.g., coronal mass ejections (CMEs) and flares). We developed HAFSS at Carmel Research Center to better characterize and utilize the solar source surface inputs. HAFSS is an improvement over HAFv2 [*Intriligator et al*., 2005].

In the HAFSS model for background SW boundary conditions (BCs) we used the WSA (Wang-Sheeley-Arge) maps [*Wang and Sheeley*, 1991; *Arge and Pizzo*, 2000]. The only boundary conditions for the HAFSS model are the distribution of V and B near the solar surface (2.5 R_S) which are obtained from NOAA's Space Weather Prediction Center (SWPC). To simulate solar activity with the HAFSS model, we applied perturbations to the background BCs. The tuning of both the background solar conditions and the solar events was iterative. The background model tuning only needed to be done once for the period of interest. In previous analyses we developed methods that made shock simulation inputs converge very quickly [*Intriligator et al*., 2015]. HAFSS itself ran quickly. Our tuning used strictly quantitative verification of model results against s/c data. That is, the input pulse magnitude (shock speed) was varied until the HAFSS-simulated 23 July shock arrival time at STEREO A (see Figure 2) was reasonably achieved. The HAFSS model's grid resolution from 2.5 R_S to 140 AU is delta (R) = 0.1 AU, delta (theta, meridional angle) = 2.5°, and delta (phi, azimuthal angle) = 2.5°. From our previous comparisons between in situ s/c observations and our HAFSS and Hybrid Heliospheric Modeling System with Pickup Protons (HHMS-PI) simulations of the propagation of solar events we have found [*Detman et al*., 2011; *Intriligator et al*., 2008, 2010, 2012] there is a mediation of pickup protons on the IP shock speed at distances of 5 AU and beyond.

Only quantitative testing of such models in a 3-D, time-dependent context against s/c data can both further validate and improve such models. We also note that HAFSS provides "quick-look" results and preliminary shock input tuning for our Hybrid Heliospheric Modeling System with Pickup Protons (HHMS-PI). HHMS-PI is our full 3-D magnetohydrodynamic time-dependent model (not used here) that includes the effects of pickup protons [*Detman et al*., 2011; *Intriligator et al*., 2012].

A full simulation model embodies the physics it contains in a directly usable form, and quantitative testing establishes benchmarks and provides feedback for further model improvement. Such simulations with robust verification can and have helped advance our understanding of important basic physical processes.

In July 2012 NOAA solar active region (AR) 1520 emitted a series of disturbances and CMEs. Table 1 summarizes the inputs for the HAFSS model of the July 2012 solar events. These characteristics of this July 2012 solar activity were obtained from the NOAA Space Weather Prediction Center (SWPC) daily Report of

Solar Geophysical Activity. In Table 1 [*Intriligator et al*., 2015] the first column is the four-digit year; the second is the four-digit month and day; the next column is the two-digit hour and the two-digit minutes of the event; the next two columns are the solar latitude and longitude of the event in the Heliocentric Earth Equatorial (HEQ) coordinate system; and VS is the shock speed (in km/s) of the event's CME's shock. The column labeled VS lists the SWPC/U.S. Air Force coronal shock speed estimates. The TAU value (in hours and minutes) is the assumed duration of the piston driving time of the coronal shocks above the flare site. Thereafter, the shape of the shock is determined by the HAFSS simulation and not by an assumed cone angle. VSW is the ambient SW speed (in km/s) at L1 (ACE); OPT is the optical magnitude of the event; and XRAY is the X-ray magnitude of the event. For the July 2012 solar events (Table 1) the NOAA listings did not include any values for the OPT and XRAY since these events occurred on the far side of the Sun. VSW was chosen as a representatively high solar wind speed (750 km/s) that followed the earlier flares [*Wu et al*., 2013]. VSW can be assumed not to vary much during a few days because it does not have a big affect on the simulation of the shock event. VS was chosen as 3603 km/s as an assumption after VS (with that value) was measured (K. Schenk, private communication, 2012) by SOHO/Large Angle and Spectrometric Coronagraph in POS (Plane of Sky).

As shown in Table 1 the largest solar event input into the HAFSS model occurred on 23 July 2012 with a VS of 3603 km/s. This solar event followed the previous solar events listed in Table 1. When the 23 July solar event was launched from the Sun it propagated through the IP that had been "swept out" by the previous solar events. Thus, the IP at this time was characterized by a lower SW plasma density than usual. It also was characterized by a radial IMF [*Baker et al*., 2013]. From our HAFSS simulations it appeared that this region of lower plasma densities propagated out to V2 in the HS at 102 AU and to V1 in the ISM at 124 AU.

To date, the HAFSS model does not include the effects of SEP mediation of the IP propagation of the solar events nor the mediation of SW shock speed. HAFSS also does not include the effects of the termination shock (TS) on the propagation of IP events from the Sun to the HS. Similarly, HAFSS does not include the effects of the HS or of the heliopause (HP) on the propagation to the ISM of these events of solar origin. To our surprise, an earlier analysis of the December 2006 solar events found that the TS was transparent to the propagation of the IP events. That is, the HAFSS model predicted the correct arrival time of the IP events at V2 even though V2 was located beyond the TS and in the HS. The implication of this result is that the TS was weak and, thus, transparent to IP events, at least with respect to observations made within an AU or so of the TS. More deceleration may occur for an IP event traveling approximately 15 AU through the HS from where the TS was observed by V2 in 2007 to where V2 was in 2013 or more than 35 AU, entirely through the HS and into the ISM, to the 2013 location of V1.

3. Analyses of HAFSS Simulations and 1 AU Spacecraft Measurements

We used HAFSS to generate predictions of the IMF configuration between the Sun and 2 AU for the background solar inputs and the solar event inputs listed in Table 1. There were a number of s/c in the inner heliosphere near 1 AU in July 2012. Also, all of these s/c were located near the ecliptic plane. However, as illustrated in the individual ecliptic plane plots in Figure 1 the s/c were widely separated in longitude (~120°).

Figure 1 shows the HAFSS predictions of the evolution in the ecliptic plane from the Sun to 2 AU of the IMF from 18 to 25 July 2012. The top left plot shows at $T = 00$ UT on 18 July 2012 the locations of the STEREO A (Sa), STEREO B (Sb) s/c and of Earth (the black dot that is not labeled), and the quiescent IMF with its toward (blue lines) and away (red lines) sectors. We note that a number of the s/c were near the radial location of the Earth at ~ L1 (e.g., ACE, Wind, and SOHO). The Sun is at the origin of these ecliptic plane plots. The top plot on the right showed that on the next day (24 h later) at $T = 00$ UT on 19 July 2012 the propagation of the event of solar origin was more discernible in the regions west of Earth. We note that the disturbance in the blue (toward) sector had not propagated as far radially as the disturbance in the red (away) sector. In the $T = 00$ UT on 21 July 2012 plot the radial propagation and evolution of several shocks is evident in three of the quadrants. The radial propagation and evolution in the ecliptic plane (to 2 AU) of the IP events of solar origin continues to be evident in the series of plots through $T = 00$ UT on 25 July 2012. It was evident that the 23 July 2012 event rapidly propagated from the Sun to 1 AU in the vicinity of STEREO A, as seen in the $T = 00$ UT 24 July plot. The $T = 00$ UT 25 July 2012 plot indicated that by this later time the 23 July solar event had propagated to 1 AU near ACE and that in the direction of STEREO A the solar event already had propagated beyond 2 AU. The sequence in Figure 1 of the HAFSS-predicted evolution from the Sun to 2 AU of

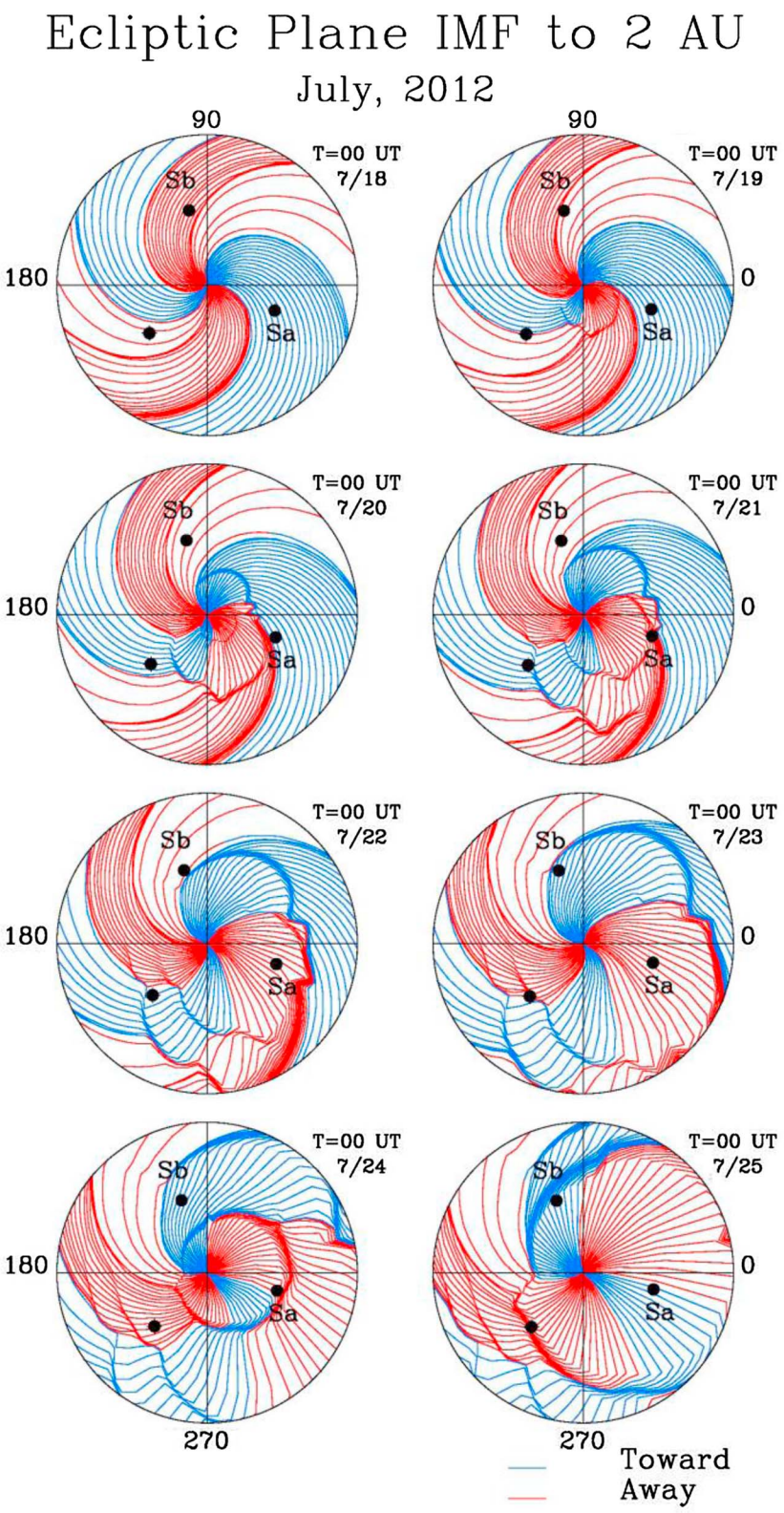

Figure 1. HAFSS simulation predictions of chronological sequence for 18 July 2012 through 25 July 2012 of ecliptic plane plots from the Sun to 2 AU. The plots show the interplanetary magnetic field (IMF) orientations and distortions associated with the ambient background solar magnetic field and the July 2012 solar events. In these ecliptic plane plots the propagation away from the Sun of the IMF distortions due to these solar events is evident. The blue (red) sectors denote that the IMF orientation is pointing toward (away from) the Sun. The locations of STEREO A, STEREO B, and Earth (unlabeled black dot) are shown (see text).

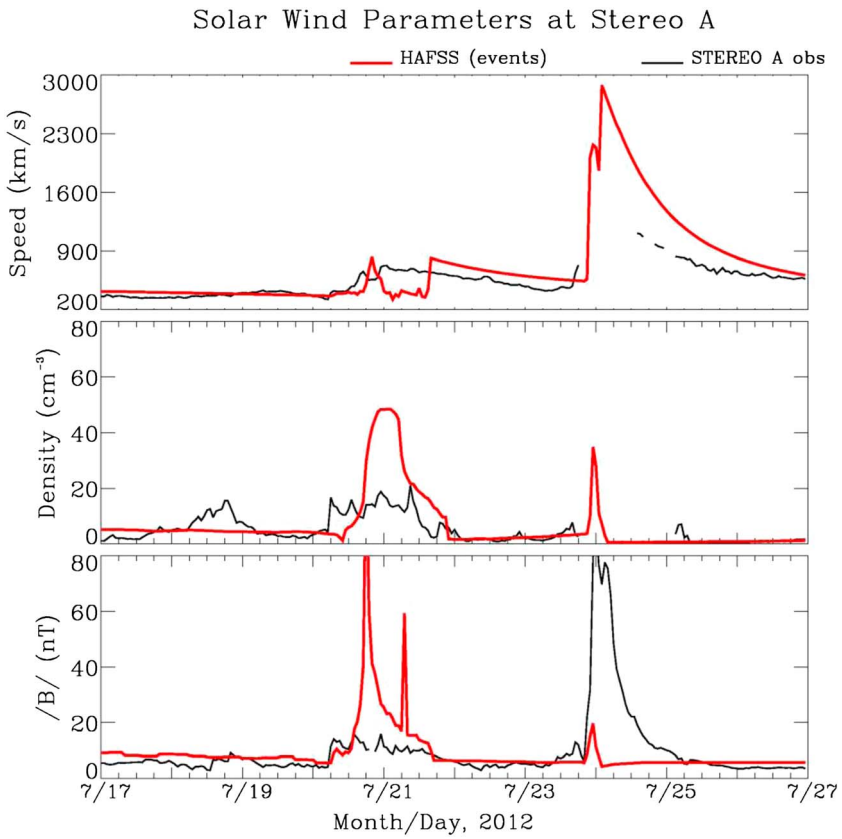

Figure 2. Comparisons of HAFSS simulations with available STEREO A observations of (top) solar wind plasma speed, (middle) density, and (bottom) IMF magnitude. The HAFSS predictions for SW plasma speed and IMF magnitude show reasonable agreement with the STEREO A observations for the initial increases on 20 July and for the large peaks at the end of 23 July and the beginning of 24 July.

the IMF from 17 to 25 July 2012 also was edifying in that it revealed the formation of various regions in the IMF, e.g., interaction regions and rarefaction regions. It is these regions, respectively, that we associate with "crests" (compressed contours at obvious simulated shocks) and "troughs" (open regions of IMF lines, hence lower IMF and SW density magnitudes) of our metaphorical "tsunami". At STEREO A the largest crest had an IMF magnitude of ~70–80 nT while the ICME was passing through this location (see Figure 2).

As indicated in Table 1 and inferred from Figure 1, the largest of the July 2012 solar events occurred at ~ 0250 UT on 23 July 2012 at west 133°, which was away from the Earth-facing side of the Sun. This solar event was approximately directed at STEREO A, whose in situ detectors measured the rapid arrival of this event. The rapid transit time was ~ 19 h [*Dryer et al*., 2012; *Baker et al*., 2013; *Liou et al*., 2014] for this event from the Sun to STEREO A. This transit time implied an average transit speed of ~ 2500 ± 500 km/s. *Liou et al*. [2014] noted from their 3-D simulation that the initial coronal shock speed was about 3100 km/s. These IP events, dramatically emphasized by this last event, prompted us to use the tsunami metaphor in the title of this paper.

Figure 2 compares the HAFSS simulation (red lines)—based on both the background ("quiescent") solar data and the solar events (Table 1)—with the STEREO A measurements (black lines). The HAFSS simulation was tuned by adjusting the 23 July solar event's shock speed (Table 1) so that the arrival time of the HAFSS-simulated 23 July shock would approximate the arrival time late on 23 July 2012 of the observed shock at STEREO A. As shown in Figure 2 prior to ~8 h before 24 July 2012 and after approximately 26 July 2012 the time series profiles of the HAFSS-predicted SW plasma speeds and the STEREO A measurements were very similar. Both the HAFSS-predicted plasma speed and the STEREO A-measured plasma speed showed a small increase near the end of 20 July 2012. Both the HAFSS simulation and the STEREO A measurements agreed on the arrival time and magnitudes of this increase. There was reasonable agreement between the arrival time of the 23 July 2012 solar event associated with the increase in the measured and HAFSS-simulated SW

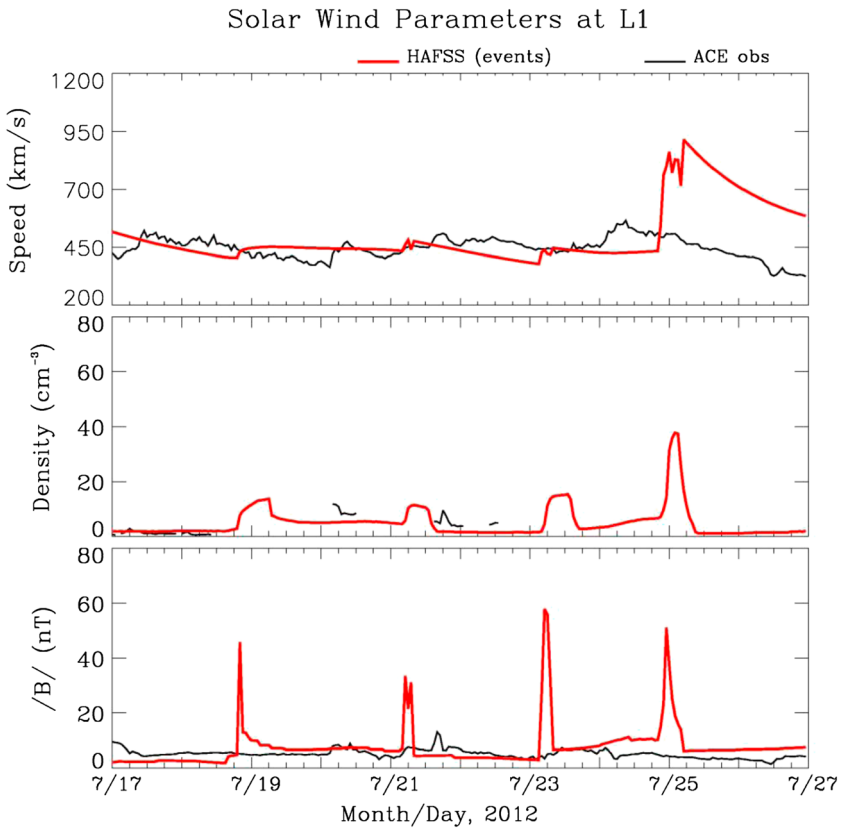

Figure 3. Comparisons of HAFSS simulations with available ACE SW plasma and IMF magnitude observations. Similar to Figure 2.

plasma speed late on 23 July 2012. The HAFSS simulation predicted that following the arrival of the event the SW plasma speed would approach ~3000 km/s. There were, unfortunately, no available STEREO A SW measurements for comparison during this time interval. For the 23 July solar events our HAFSS-simulated results for the plasma speed and density agree with those of *Liou et al*. [2014].

Comparison of the HAFSS-simulated and STEREO A-measured density profiles showed two distinct events. There was some agreement between the arrival time of the approximately 20 July 2012 solar event density increase in both the HAFSS-simulated plasma density and the STEREO A-measured plasma density. STEREO A measured a plasma density increase on 20 July 2012 ~ 12 h earlier than that predicted by HAFSS. Also, the magnitude of the STEREO A-measured peak plasma density was $\lesssim 20\,\mathrm{cm}^{-3}$ in contrast to the HAFSS-simulated plasma density of $> 40\,\mathrm{cm}^{-3}$. STEREO A also measured an increase in plasma density on 18 July 2012, whereas the HAFSS simulation did not predict a plasma density increase before the plasma density increase at the end of 20 July 2012 discussed above. The HAFSS simulation predicted that there would be a plasma density increase late on 23 July 2012 associated with the large shock arrival shown in the HAFSS-predicted SW plasma speed. As in the case of the STEREO A plasma speed measurements discussed above, there are no STEREO A plasma density measurements available during the apparent arrival of the large shock at STEREO A. We note that the STEREO A IMF data, shown in Figure 2 (bottom), supported the HAFSS simulation result that a major shock arrived at STEREO A during this time interval when no STEREO A SW plasma data were available. We associated the large speed, density, and IMF magnitude increases (e.g., peaks and crests) late on 23 July 2012 with the arrival at STEREO A of the metaphorical tsunami from the 23 July 2012 solar event (Table 1). This unusually fast arrival time at 1 AU was due to the magnitude of the 23 July 12 solar event, its solar launching in the approximate direction of STEREO A, and its very high initial shock speed of 3603 km/s (Table 1) and also probably in part to the IP rarefaction region (i.e., the minimum and trough) in the SW speed and density (Figure 2) that preceded the transit of the 23 July 2012 solar event.

Figure 3 shows the comparisons from 17 to 27 July 2012 near L1 between the HAFSS simulation (red line) of the July 2012 solar events and the ACE plasma and IMF magnitude measurements (black lines). As shown in

Figure 1 and discussed above, ACE was located at 1 AU ~ 120° away from STEREO A and the 23 July 2012 flare site. The HAFSS simulation was based on both the background solar conditions and the solar events listed in Table 1. Figure 3 (top) shows the HAFSS-predicted and the ACE-measured SW plasma speed. Before approximately 24 July 2012 there was relatively good agreement between the HAFSS-predicted plasma speed and the ACE-measured plasma speed in this speed profile as a function of time. Figure 3 (top) the HAFSS comparisons with ACE plasma data show that the highest HAFSS-simulated SW plasma speed, which was associated with the arrival at ACE of the 23 July solar event, had a higher magnitude (~900 km/s) than the peak-measured plasma speed ($\lesssim$600 km/s) at ACE. Figure 3 (middle) shows the HAFSS-predicted plasma density and the plasma density measured on ACE. The measured peak density never exceeded ~10 cm^{-3}. HAFSS predicted four distinct plasma density increases which occurred near approximately 19, 21, 23, and 25 July. The highest HAFSS-predicted plasma density peak magnitude was ~40 cm^{-3} and was associated with the HAFSS-predicted increase in plasma speed (Figure 3 (top)) on approximately 25 July (late 24 July) due to the arrival at ACE of the large 23 July solar event. Figure 3 (bottom) shows the comparison between the HAFSS simulation and the ACE IMF magnitude data. The measured ACE IMF magnitude does not show a peak coincident with the HAFSS manifestation of the arrival of the 23 July 2012 solar event at ACE. The timing of the arrival of the HAFSS-simulated IMF magnitude peak is approximately coincident with the HAFSS arrival of the speed and density peaks associated with the 23 July 2012 solar event.

Continuing our analogy to the metaphorical tsunami, we also associate it with this remarkable shock expansion around the Sun and arrival at ACE. We associate the HAFSS-predicted maxima in plasma speed, density, and IMF magnitude with the crest of the tsunami and its arrival at ACE.

As discussed in section 1, *Mewaldt* [2014] and others have shown that the 23 July shock as observed at STEREO A and ACE was mediated by the SEPs associated with the 23 July solar event. The HAFSS-predicted speed and density time profiles shown in Figures 2 and 3 do not take this SEP mediation into account.

4. Analyses of HAFSS Simulations and Voyager Spacecraft Measurements

In this section we will be comparing the HAFSS simulations with V1 and V2 available data in two scenarios: (1) simulation to V2 that extends to December 2013 with the assumption that the above tsunami had taken place and (2) simulation to V1 with the same assumption.

4.1. Simulation in HEQ System Until December 2013 and Then With Coordinate Transformation Requirement: Voyager 2

Unlike the s/c near 1 AU, the V1 and V2 s/c were not located near the ecliptic plane. Also, V1 and V2 were not located in the inner heliosphere close to the Sun, rather they were located at 124 AU and 102 AU, respectively, which was beyond the outer heliosphere and beyond the TS. In July 2012 both V1 and V2 were in the HS. In fact, as would be evident in the V1 data about 1 month later, V1 was crossed by the HP on 25 August 2012 and entered the ISM at that time [*Webber and McDonald*, 2013]. V1 was located at +34° (34°N of the ecliptic plane). V2 was located at −30° (30°S of the ecliptic plane).

For comparison with Figure 1, Figures 4a and 4b show the HAFSS prediction of the July 2012 IMF disturbances in the HEQ ecliptic plane out to 140 AU on 1 June 2013 and on 28 December 2013, respectively. The locations of the V1 and V2 s/c projected on the ecliptic plane were indicated in these figures at longitudes of ~ 174° and 217°, respectively. As in Figure 1, in Figures 4a and 4b the "toward" and "away" orientations of the IMF were denoted by the blue and red lines, respectively. The plot in Figure 4a indicates that the HAFSS simulation predicts that if on 1 June 2013 V2 (at 102 AU and at ~ 217° longitude) had been located in the HEQ ecliptic plane (rather than 30°S), V2 would have been in the vicinity of the "shock" associated with the July 2012 solar events. The shock could have been a merged interaction region (MIR) or a global MIR (GMIR). In Figure 4a the HAFSS simulation also predicts that on 1 June 2013 there was no disturbance in the vicinity of V1 associated with the July 2012 solar events.

In Figure 4a the simulation indicates that by 1 June 2013 the IP manifestation of the July 2012 solar events probably had propagated up to or beyond the radial location of V2 in the ecliptic plane. V2 appeared to be near a boundary region between the more intense magnetic fields and the magnetic fields of very low strength. Figure 4b is similar to Figure 4a and indicates the HAFSS simulation of the July 2012 solar events to 140 AU in the ecliptic plane on 28 December 2013. In contrast to Figure 4a, Figure 4b implies that on 28

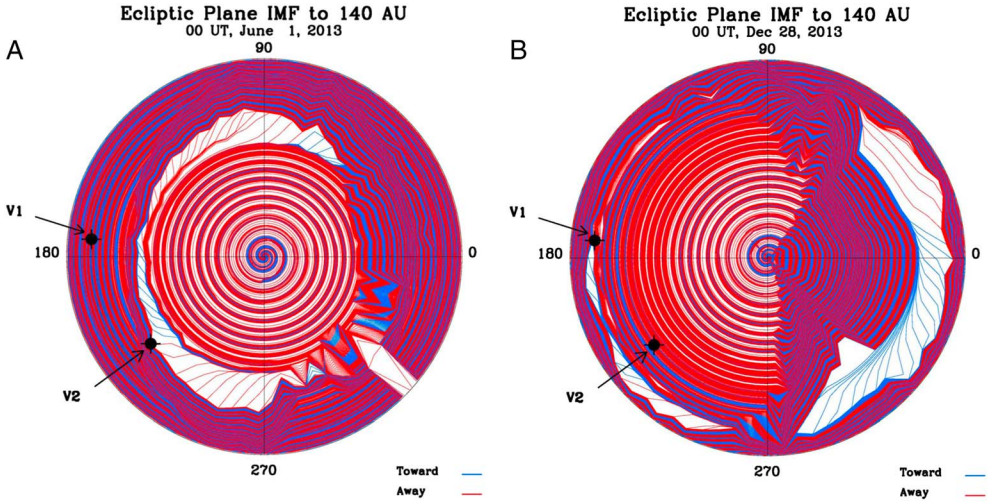

Figure 4. (a and b) Similar to Figure 1 showing the HAFSS simulation in the ecliptic plane of the IMF from the Sun to 140 AU on 1 June 2013 and on 28 December 2013, respectively. The locations of V1 and V2 are shown (see text).

December 2013 if V1 were actually located in the ecliptic plane at 123 AU and at ~ 174° longitude the July 2012 solar disturbances would have propagated to the vicinity of V1. In Figure 4b the HAFSS simulation also predicts that the IP events associated with the July 2012 solar events would have propagated beyond the radial distance of V2 at this time. V2 appeared to be immersed in a region of large magnetic fields, while V1 appeared to be located in a low intensity magnetic field boundary region between two regions of enhanced magnetic fields. As in the plots in Figure 1, the HAFSS modeled ecliptic plane IMF plots in Figures 4a and 4b are useful for determining the various regions in the magnetic field, i.e., the interaction regions, the spiral field regions, the rarefaction regions, the regions of radial fields, and the GMIRs. As discussed above, in connection with our tsunami metaphor we associated some of these regions (e.g., interaction regions and the GMIRs) with the tsunami peaks/crests and other regions (e.g., the rarefaction regions) with the tsunami minima/troughs.

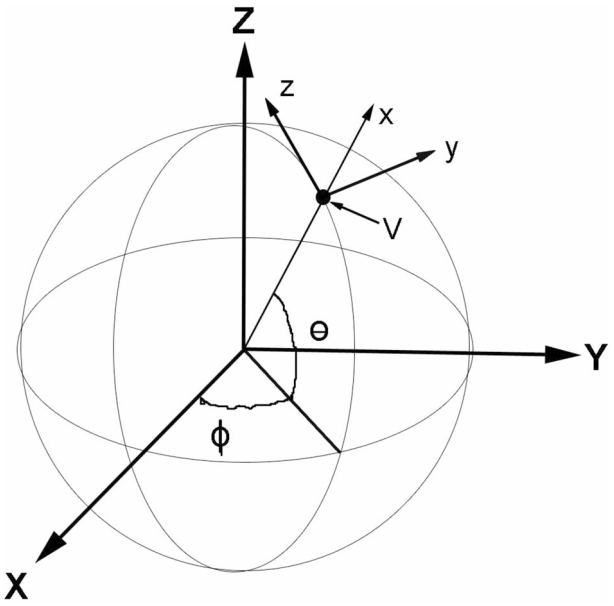

Coordinate transformation, where

$x = X\,\mathrm{Cos}\Theta\,\mathrm{Cos}\Phi + Y\,\mathrm{Cos}\Theta\,\mathrm{Sin}\Phi + Z\,\mathrm{Sin}\Theta$

$y = -X\,\mathrm{Sin}\Phi + Y\,\mathrm{Cos}\Phi$

$z = -X\,\mathrm{Sin}\Theta\,\mathrm{Cos}\Phi - Y\,\mathrm{Sin}\Theta\,\mathrm{Sin}\Phi + Z\,\mathrm{Cos}\Theta$

Figure 5. Coordinate transformation used for V1 and V2 since, respectively, their latitudes are +34° (north) and −30° (south) of the ecliptic plane (see text).

The HEQ discussion above is only an initial approximation to the predictions for V1 and V2 because these s/c are so far above and below the ecliptic plane, respectively. For each s/c the coordinate systems must be changed to the respective *xyz* systems, according to the formulas in Figure 5, for appropriate comparisons between the available data and the HAFSS simulation, which is strongly *nonspherically symmetric*. This requirement is now discussed.

As discussed at the beginning of this section, V2 and V1 were not located

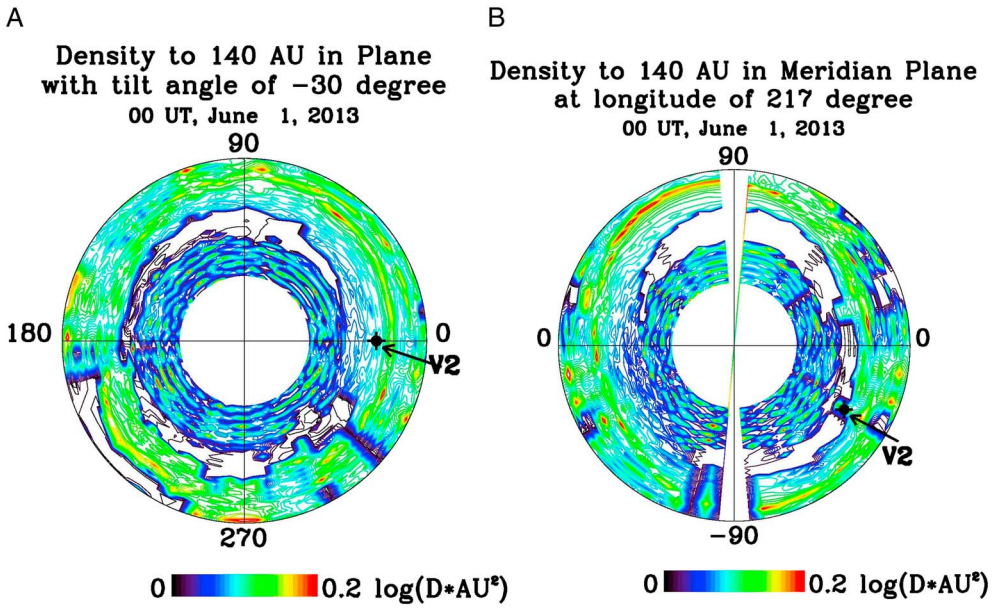

Figure 6. (a) HAFSS-simulated plasma density to 140 AU in the tilted plane (30°S) for V2 on 1 June 2013 (see text). (b) HAFSS-simulated plasma density to 140 AU in V2 meridian plane to 140 AU on 1 June 2013.

in the ecliptic plane. V2 was located at 30°S and V1 was located at 34°N. In order to more accurately determine the IP effects and manifestations of the July 2012 solar events at each of these s/c we employed a coordinate transformation and applied it to each of these s/c. Figure 5 shows the coordinate transformation. In the HAFSS code all calculations of speed, density, and magnetic field are in HEQ coordinates so that longitude in the ecliptic plane plots (i.e., Figures 1 and 4) or in tilted plane plots should be in HEQ coordinates. The HEQ coordinate system is shown by *XYZ* in Figure 5.

A new coordinate system is designated as the *xyz* system at point V (location of Voyager). The tilt angle of the *xy* plane to the *XY* plane is the Θ angle. The difference in longitude between *XYZ* and *xyz* system is the angle Φ.

Figures 6a and 6b are similar in format to Figures 4a and 4b and show the HAFSS-simulated plasma density out to 140 AU. However, unlike the previous radial plots for Figures 6a and 6b we made the coordinate transformation for V1 and V2 by putting the respective s/c latitudes and longitudes into the formulas in Figure 5. Also rather than showing the IMF, Figures 6a and 6b show the plasma density. Thus, Figure 6a shows for 1 June 2013 the HAFSS-simulated plasma density from the Sun to 140 AU in the V2 plane with the tilt angle of 30°S. In this *xyz* coordinate system the 0 axis is the radius from the Sun to V2. The reader is reminded that the solar events noted earlier in section 2 are considered in the HAFSS simulation.

Figure 6a thus improved on Figures 4a and 4b and showed how the July 2012 solar disturbances propagated out to 140 AU from the Sun in the tilted plane 30°S of the ecliptic plane that corresponded to the actual location of V2. Figure 6a implied that approximately 1 June 2013 V2 appeared to be in a region of low plasma densities. At distances of $R > R_{V2}$ there appeared to be more enhanced plasma density. At distances of $R < R_{V2}$ near V2 there appeared to be region of very low plasma density. Moving farther inward toward the Sun, there appeared to be a region of more enhanced plasma density or perhaps a region composed of islands of more enhanced plasma density. Figure 6b showed for 1 June 2013 the HAFSS simulated plasma density out to 140 AU in the meridian plane at a longitude of 217°, which is the longitude of V2. Figure 6b depicts an estimate that V2 was in a region of enhanced plasma densities. Figure 6b may have further implied that this region of enhanced plasma densities was bordered in longitude by regions of extremely depressed plasma densities or an absence of plasma. In the vicinity of V2 in the radial region inward ($R < R_{V2}$) there appeared to be near V2 first an enhancement in plasma density and adjacent to that enhancement region a small region with an absence of plasma. Continuing inward along the V2 radial line the model estimated that a much larger region of enhanced plasma densities or islands of enhanced plasma densities was present.

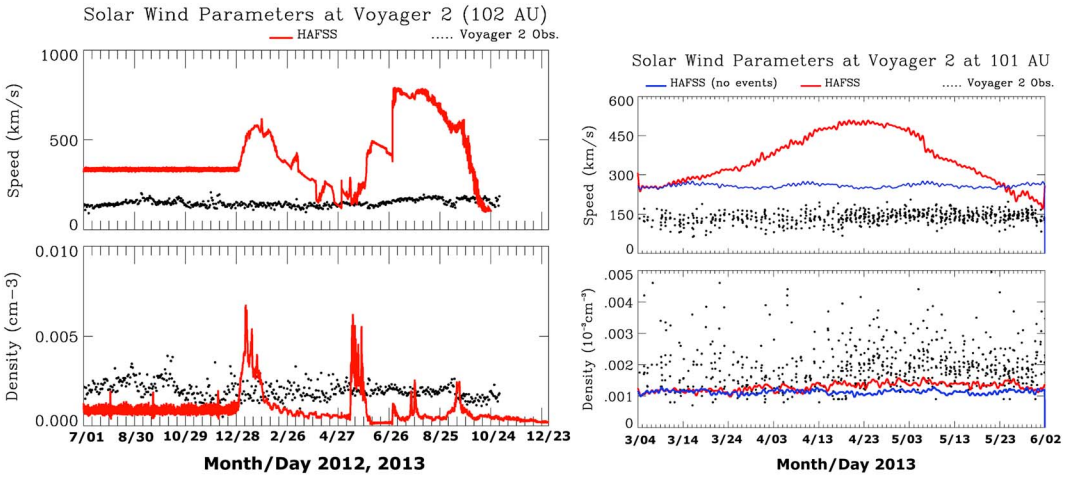

Figure 7. (a) Comparisons for 1 July 2012 to 23 December 2013 of HAFSS time series simulations at V2 with the measured in situ (top) plasma speed and (bottom) density. (b) Comparisons for 4 March 2013 to 2 June 2013 of HAFSS time series simulations at V2 with the measured in situ (top) plasma speed and (bottom) density. The red (blue) lines denote HAFSS simulations include (exclude) solar event inputs (Table 1).

In contrast moving outward along the V2 radial line it appeared that V2 was bordered by a region with plasma that was generally denser than the region closer to the Sun. As in Figures 1 and 4a and 4b the various global regions are revealed in Figures 6a and 6b. As discussed above the global variations in the plasma density are evident in Figures 6a and 6b. The global configurations of the regions of enhanced plasma densities, rarefied plasma density, etc., are reminiscent of the configuration of GMIRs, etc. Here again we associated the regions of GMIRs and enhanced plasma densities with the peaks/crests of the tsunami and the rarefaction regions and depleted plasma densities with the minima/troughs of the tsunami.

Figures 7a and 7b are similar to Figure 2. Figures 7a and 7b compare the HAFSS simulation time series results (red lines) for the July 2012 solar events (Table 1) with the V2 plasma data (black dots). Figure 7a covered the time interval from 1 July 2012 to approximately 23 December 2013. During this time interval the V2-measured plasma speed (Figure 7a (top)) was near ~150 km/s. As shown in Figure 7a, HAFSS predicted that the plasma speed would be steady near ~375 km/s from the beginning of this time interval until approximately 28 Decemeber 2013. Following this, the HAFSS-predicted time profile of the plasma speed showed two broad peaks (crests) with a speed dip (trough) between them. HAFSS predicted that the first speed peak/crest occurred near 28 December 2012 and continued until approximately 26 February 2013. The magnitude of this first speed peak/crest was ~600 km/s. Following this peak/crest in the HAFSS-predicted speed, the HAFSS-predicted speed decreased to a minimum speed (trough) near ~150 km/s, which was approximately the same speed as the measured plasma speed. HAFSS also predicted that during the time interval from near the end of February 2013 to when the plasma speed was decreasing there would be some additional variations in speed in April/May 2013. The magnitude of these variations was ~100–200 km/s. One of these variations is described below (Figure 7b). Following this trough, HAFSS predicted a larger magnitude speed peak/crest with longer duration that started near approximately 1 June 2013 and continued until almost 24 October 2013. The highest speed magnitude associated with this second HAFSS-predicted speed peak/crest was ~800 km/s. Figure 7a (top) also shows that the V2 plasma analyzer did not measure (black dots) any substantial peaks in the plasma speed during the entire time interval from 1 July 2012 to approximately 1 November 2013. HAFSS also predicted that associated with the July 2012 solar events (Table 1) there were two associated density peaks/crests (Figure 7a (bottom)) of higher magnitude starting near 28 December 2012 and near 12 May 2013. The duration of the HAFSS-predicted first large density peak/crest was ~30 days. The duration of the HAFSS-predicted second large density peak/crest was ~20 days. Between these two HAFSS-predicted large density peaks/crests HAFSS predicted a prolonged density minimum/trough. HAFSS also predicted three smaller density peaks/crests starting near 26 June 2013, 26 July 2013, and 4 September 2013. As compared with the V2-measured plasma speeds, the time profile of the V2-measured plasma densities was more similar to the HAFSS plasma density predictions. Both the

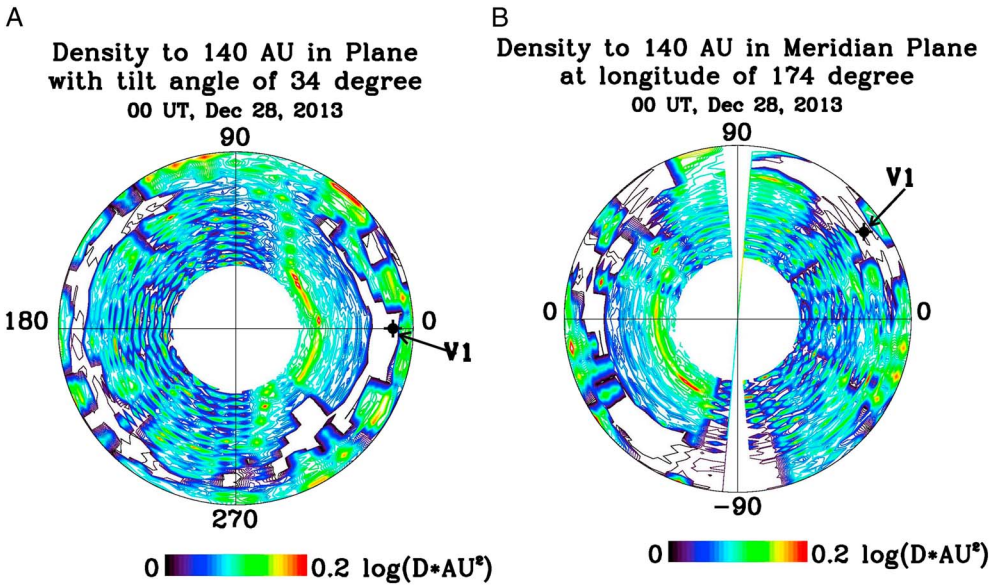

Figure 8. (a) HAFSS-simulated plasma density to 140 AU in tilted plane (34°N) for V1 on 28 December 2013. (b) HAFSS-simulated plasma density to 140 AU in V1 meridian plane on 28 December 2013.

HAFSS-simulated and V2-measured plasma densities showed a series of peaks. The magnitudes of the HAFSS-predicted density peaks/crests were larger than those measured by the V2 Plasma Subsystem (PLS) instrument. Also, the two larger PLS-measured peaks/crests appeared to perhaps lead the two larger predicted HAFSS density peaks/crests. We associate (a) the plasma speed peaks/crests and density peaks/crests with MIRS and GMIRS and (b) the plasma speed minima/troughs and density/troughs with rarefaction regions.

Figure 7b is similar to Figure 7a. It compares the time series of the HAFSS plasma simulations with the V2-measured data for a portion of the time interval shown in Figure 7a. Figure 7b covered the time interval from 4 March 2013 to 2 June 2013. Figure 7b shows the results of two HAFSS simulations. Unlike all the previous HAFSS simulations shown above the first HAFSS simulation (blue lines) in Figure 7b shows the HAFSS predictions based on including only the background solar inputs (the quiescent solar inputs) and excluding the solar events listed in Table 1. As in the case of all the HAFSS simulations shown in previous figures, the second HAFSS simulation (red lines) shows the HAFSS-predicted results when all the solar events listed in Table 1 also were included. The V2 data (black dots) are used to show the PLS-measured plasma speed and density. From Figure 7b it was evident that HAFSS using only the background solar data and excluding the solar event inputs predicted (blue lines) that both the V2 plasma speed and density would show no substantial variations. In contrast, the HAFSS predictions (red line) based on both the background solar data and the solar events listed in Table 1 showed a plasma speed increase from less than ~300 km/s to more than 450 km/s during this time interval. The HAFSS-predicted plasma speed increase began approximately 23 March 2013 and lasted until almost the end of May 2013. A corresponding plasma density increase of very small magnitude was predicted (red line) starting in April 2013.

The HAFSS time series predictions for V2 shown in Figures 7a and 7b correlated with the simultaneous V2 Cosmic Ray Subsystem (CRS) measurements. These will be discussed in a separate paper.

4.2. Simulation Until December 2013 With Coordinate Transformation Requirement: Voyager 1

Figures 8a and 8b are similar to Figures 6a and 6b. Figure 8a shows for 28 December 2013 the HAFSS-simulated plasma density from the Sun to 140 AU in the V1 plane with the tilt angle of 34°N of the ecliptic plane corresponding to the actual location of V1. In this *xyz* coordinate system the 0 axis is the radius from the Sun to V1. In Figure 8a HAFSS predicted that approximately 28 December 2013 V1 was in a region with an absence of plasma. This region with very low density plasma or with an absence of plasma appeared to be quite large. Here again we associate these minima/rarefaction regions with the troughs in our tsunami metaphor. In the radial direction of V1 this depleted plasma region appeared to extend over many astronomical units, particularly at radial distances less than that of V1.

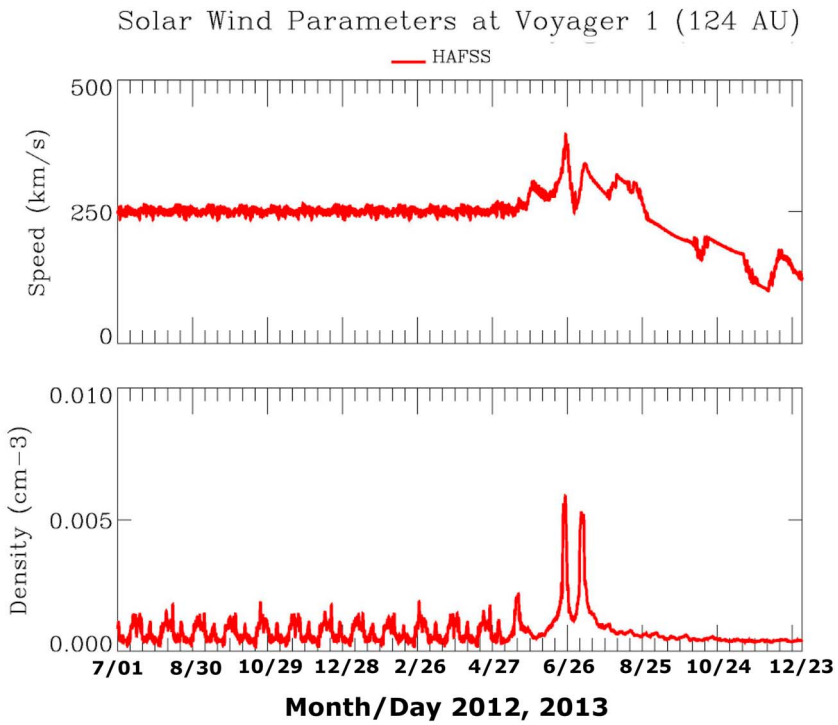

Figure 9. V1 time series plots 1 July 2012 to 23 December 2013 of HAFSS-simulated (top) plasma speed and (bottom) density. There are no available V1 plasma data for comparison since the V1 plasma instrument (PLS) stopped operating in 1980.

In Figure 8a HAFSS also predicted that a region of enhanced plasma density may have propagated beyond the radial location of V1. We associated this density maxima/GMIR region with the tsunami crest. In the longitudinal direction HAFSS predicted that the depleted plasma rarefaction/trough region also was larger extending over many degrees in longitude. In Figure 8a HAFSS predicted that there also was a large region of enhanced plasma density (the crest) much closer to the Sun along the radial line to V1. As in Figures 6a and 6b, the global configurations of the HAFSS-predicted plasma density in Figure 8a appeared to emphasize the GMIRs (the crests) and the global nature of the very low plasma density rarefaction regions (the troughs), etc. From Figure 8b it was tempting to conclude that by 28 December 2013 in V1's meridian plane V1 was in a region with mainly an absence of plasma (a rarefaction/trough region) while a large region of enhanced plasma densities (a GMIR/crest region) was approaching V1 from the sunward direction. From Figure 8b it also appeared that another GMIR/crest region of enhanced plasma density already had propagated beyond the radial location of V1.

Figure 9 shows the HAFSS simulation results predicted for the V1 plasma at 124 AU. Unfortunately, there were no V1 plasma data available since the V1 PLS plasma instrument stopped operating in 1980. Figure 9 covers the time interval from 1 July 2012 to 23 December 2013. In Figure 9 HAFSS predicted that the time profile of the plasma speed (Figure 9 (top)) was near ~250 km/s from 1 July 2012 until early June 2013. HAFSS predicted that the plasma speed began to increase in early June 2013 and reached a peak near ~400 km/s on approximately 26 June 2013. HAFSS predicted that following this peak the plasma speed underwent a generally downward trend, interspersed with some relatively short time intervals of speed increases. On 23 December 2013 the HAFSS-predicted plasma speed magnitude was ~125 km/s. HAFSS also predicted two associated density peaks (Figure 9 (bottom)) near 26 June 2013, the time of the predicted speed peak. From 1 July, 2012 to approximately late May 2013 HAFSS predicted that the plasma density was ~0.001 cm^{-3} or less. Following this HAFSS predicted that there were three density peaks. The first density peak, with its small increase in magnitude, preceded the HAFSS-predicted first small speed increase in Figure 9 (top). The next HAFSS density peak, the largest (>0.005 cm^{-3}), preceded the largest HAFSS speed predicted. The third (last) HAFSS density peak (~0.005) predicted also was

associated with a HAFSS-predicted speed peak. Following these three HAFSS-predicted density peaks, the predicted plasma density gradually decreased to its lowest magnitude (slightly greater than 0.000 cm^{-3}). In this HAFSS prediction this region of low plasma density was different from the region of low plasma density that preceded all three of the density peaks. Prior to the three density peaks, HAFSS predicted an oscillatory behavior in the plasma density. HAFSS also predicted a less pronounced oscillatory behavior in the associated speed variations during this earlier time (1 July 2012 to approximately late May 2013). The HP crossing of V1 occurred on 25 August 2012 [*Webber and McDonald*, 2013]. The correlations between the HAFSS predictions and the V1 cosmic ray data in the HS and in the ISM will be discussed in another paper.

5. Discussion and Conclusions

Our HAFSS simulations start near the Sun at 2.5 R_S with both the quiescent background solar conditions and the solar events (Table 1) as inputs. The HAFSS simulations then propagate outward where we compared the HAFSS predictions with the in situ s/c measurements. Based on these comparisons, it was tempting to conclude that the July 2012 solar events did cause a tsunami in the plasma and magnetic field throughout the heliosphere, HS, and into the ISM. Our HAFSS simulations showed evidence of interaction regions and rarefaction regions in the inner heliosphere (1 AU) and of GMIRs and rarefaction regions in the HS and ISM. The crests (e.g., interaction regions, MIRs, and GMIRs) and troughs (e.g., rarefaction regions) in the heliosphere, HS, and ISM are similar to those associated with the tsunami water/wave crests and troughs.

Solar events can adversely impact space weather in the vicinity of Earth [*Akasofu*, 2011; *Baker et al*., 2013; *Ngwira et al*., 2013]. There was a rapid transit of the 23 July 2012 shock from the Sun to STEREO A, which was located at 1 AU in the longitudinal vicinity of the solar source region of the 23 July 2012 solar event (Table 1). The 23 July 2012 solar event was particularly interesting since at STEREO A it appeared to be comparable to or stronger than the 1859 Carrington event. This extreme 23 July 2012 major solar event occurred on the farside of the Sun and thus was not visible from Earth. In this present paper we used the 3-D time-dependent HAFSS kinematic model to simulate the IP impacts of the 17–23 July 2012 solar events at 1 AU at two widely spaced longitudes. We compared these HAFSS predictions with STEREO A and ACE SW plasma measurements. At 1 AU *Mewaldt* [2014] and others presented evidence of the July 2012 solar events' impacts from solar energetic particles (SEPs) on the plasma, IMF, and evolution of the propagation of the solar events. At 1 AU the SEPs from the July 2012 events impacted the plasma and IMF and mediated the propagating shock.

We also employed HAFSS to simulate the propagation of the quiescent solar conditions and of the July 2012 solar events from the Sun to the HS and ISM. We compared our HAFSS predictions with the available in situ plasma measurements at V2 and V1. Based on our analyses we concluded that there appeared to be evidence that the affects of these July 2012 solar events propagated to the vicinity of V2 and V1. In July 2012 these Voyager s/c were located in the HS out of the ecliptic plane at 30°S (V2) and 34°N (V1).

From comparisons with our HAFSS simulations of the plasma with the measured CRS energetic particle data there appeared to be evidence that impacts of the July 2012 solar events also affected the CRS-measured energetic particles at V2 and V1. These correlations between the HAFSS predictions and the V2 and V1 CRS measurements will be discussed in a separate paper.

In previous work with the HAFSS model *Intriligator et al*. [2015] used the HAFSS simulations to analyze the impacts of the March 2012 solar events at 1 AU in the vicinity of Earth, V2, and V1. They concluded that the March 2012 solar events appeared to be responsible for the enhanced 2–3 kHz PWS signals on V1 in April/May 2013. All of the March 2012 solar events occurred at northern latitudes on the Sun. In contrast, the July 2012 solar events primarily occurred at southern latitudes.

We cannot overemphasize the fact that global nonsymmetric IP response to solar events, such as the metaphorical tsunami discussed here, requires inner heliospheric confirmation. It also requires appropriate coordinate transformations for s/c plasma and IMF theory/data comparisons as exemplified by the V1 and V2 analyses discussed here.

Acknowledgments
We are indebted to NASA, NOAA (http://www.swpc.noaa.gov/products/report-and-forecast-solar-and-geophysical-activity), the NSSDC (http://nssdc.gsfc.nasa.gov/), and the ACE (http://www.srl.caltech.edu/ACE/ASC/DATA/level3/mag/magswesummary.cgi?LATEST=0&YEAR=2012&MONTH=07&DAY=27&DOY=−1), STEREO (ftp://spdf.gsfc.nasa.gov/pub/data/stereo/ahead/coho1hr_magplasma/2012/), and Voyager (ftp://spdf.gsfc.nasa.gov/pub/data/voyager/voyager2/merged/vy2_2012.asc) projects for making their data available. This work was supported in part by Carmel Research Center, Inc. The authors thank the original two reviewers for their constructive comments.

Yuming Wang thanks three reviewers for their assistance in evaluating this paper.

References

Akasofu, S.-I. (2011), A historical review of the geomagnetic storm-producing plasma flows from the Sun, *Space Sci. Rev.*, *164*, 85–132.

Arge, C. N., and V. J. Pizzo (2000), Improvement in the prediction of solar wind conditions using near-real time solar magnetic field updates, *J. Geophys. Res.*, *105*, 10,465–10,479, doi:10.1029/1999JA000262.

Baker, D. N., X. Li, A. Pulkkinen, C. M. Ngwira, M. L. Mays, A. B. Galvin, and K. D. C. Simunac (2013), A major solar eruptive event in July 2012: Defining extreme space weather scenarios, *Space Weather*, *11*, 585–591, doi:10.1002/swe.20097.

Detman, T. R., D. S. Intriligator, M. Dryer, W. Sun, C. S. Deehr, and J. Intriligator (2011), The Influence of pickup protons, from interstellar neutral hydrogen, on the propagation of the Halloween 2003 solar events to ACE and Ulysses: A 3-D MHD modelings study, *J. Geophys. Res.*, *116*, A03105, doi:10.1029/2010JA015803.

Dryer, M., K. Liou, C.-C. Wu, S.-T. Wu, N. Rich, S. Plunkett, L. Simpson, C. D. Fry, and K. Schenk (2012), Extreme fast coronal mass ejection on 23 July 2012, Abstract SH44B-04 presented at 2012 AGU Fall meeting, San Francisco, Calif., 3–7 Dec. 2012.

Florinski, V., R. B. Decker, J. A. le Roux, and G. P. Zank (2009), An energetic-particle-mediated termination shock observed by Voyager 2, *Geophys. Res. Lett.*, *36*, L12101, doi:10.1029/2009GL038423.

Howard, R. A., et al. (2008), Improvement in the prediction of solar wind conditions using near-real time solar magnetic field update, *Space Sci. Rev.*, *136*, 67–115.

Intriligator, D. S., W. Sun, M. Dryer, C. D. Fry, C. Deehr, and J. Intriligator (2005), From the Sun to the outer heliosphere: Modeling and analyses of the interplanetary propagation of the October/November (Halloween) 2003 solar events, *J. Geophys. Res.*, *110*, A09S10, doi:10.1029/2004JA010939.

Intriligator, D. S., et al. (2008), Particle acceleration and transport in the heliosphere and beyond, *7th Annual International Astrophysics Conference, AIP Conf. Proc., 1039*, edited by G. Li et al., pp. 375–383, Kauai, Hawaii.

Intriligator, D. S., et al. (2010), Voyager 2 high energy ions near the outward moving termination shock, *9th Annual International Astrophysics Conference, AIP Conf. Proc., 1352*, edited by Le Roux et al., pp. 148–157, Maui, Hawaii.

Intriligator, D. S., T. Detman, G. Gloecker, C. Gloeckler, M. Dryer, W. Sun, J. Intriligator, and C. Deehr (2012), Pickup protons: Comparisons using the three-dimensional MHD HHMS-PI model and Ulysses SWICS measurements, *J. Geophys. Res.*, *117*, A06104, doi:10.1029/2011JA017424.

Intriligator, D. S., et al. (2015), *13th Annual International Astrophysics Conference, Voyager, IBEX, and the Interstellar Medium*, *Conf. Ser.*, edited by G. P. Zank, 251 pp., IOP, Mrytle Beach, S. C.

Liou, K., C.-C. Wu, M. Dryer, S.-T. Wu, N. Rich, S. Plunkett, L. Simpson, C. D. Fry, and K. Schenk (2014), Global simulation of extremely fast coronal mass ejection on 23 July 2012, *J. Atmos. Sol. Terr. Phys.*, *121*, 32–41, doi:10.1016/j.jastp.2014.09.13.

McComas, D., N. Angold, H. A. Elliott, G. Livadiotis, N. A. Schwadron, R. M. Skoug, and C. W. Smith (2013), Weakest solar wind of the space age and the current "mini" solar max, *Astrophys. J.*, *779*, 2, doi:10.1088/0004-637x/779/1/2.

Mewaldt, R. (2014), Solar proton events of solar cycle 24 Space Weather Week.

Ngwira, C. M., A. Pulkkinen, L. Mays, et al. (2013), Simulation of the 23 July 2012 extreme space weather event: What if this extremely rare CME was Earth directed?, *Space Weather*, *11*, 671–679, doi:10.1002/2013SW000990.

Russell, C. T., et al. (2013), The very unusual interplanetary coronal mass ejection of 2012 July 23: A blast wave mediated by solar energetic particles, *Astrophys. J.*, *770*, 38.

Shen, F., C. Shen, J. Zhang, P. Hess, Y. Wang, X. Feng, H. Cheng, and Y. Yang (2014), Evolution of the 12 July 2012 CME from the Sun to the Earth: Data constrained three-dimensional MHD simulations, *J. Geophys. Res. Space Physics*, *119*, 7128–7141, doi:10.1002/2014JA020365.

Wang, Y.-M., and N. R. Sheeley Jr. (1991), Magnetic flux transport and the sun's dipole moment: New twists to the Babcock-Leighton model, *Astrophys. J.*, *372*, L45–L48.

Webber, W. R., and F. B. McDonald (2013), Recent Voyager 1 data indicate that on 25 August 2012 at a distance of 121.7 AU from the Sun, sudden and unprecedented intensity changes were observed in anomalous and galactic cosmic rays, *Geophys. Res. Lett.*, *40*, 1665–1668, doi:10.1002/grl.50383.

Wu, S. T., et al. (2013), Analyses of the evolution and interaction of multiple coronal mass ejections and their shocks in July 2012, in *12th Annual International Astrophysics Conference, Outstanding Problems in Heliophysics: From Coronal Heating to the Edge of the Heliosphere*, edited by Q. Hu and G. P. Zank, pp. 232–238, Myrtle Beach, S. C.